

Topological properties of magnetically ordered heavy-fermion systems in the presence of mirror symmetry

¹Kazuhiro KIMURA*,^{1,2}Tsuneya YOSHIDA, and ¹Norio KAWAKAMI

¹*Department of Physics, Kyoto University, Kyoto 606-8502, Japan*

²*Division of Physics, Tsukuba University, Tsukuba, Ibaraki 305-8571, Japan*

We explore topological states with magnetic order in heavy-fermion systems by taking account of a mirror symmetry. Although without spatial symmetry, there is no topological phase in the two-dimensional (2D) antiferromagnetic phases at half filling, we demonstrate that a topological phase emerges in the presence of mirror symmetry. This is explicitly shown for a two-dimensional periodic Anderson model. Furthermore, our analysis around quarter filling shows that a half-metallic state emerges in the ferromagnetic phase, where a spin-selective gap opens, resulting in nontrivial properties characterized by a Chern number. In contrast to the previously proposed models, our scenario can apply even for spin nonconserving systems in the presence of spin-orbit coupling.

KEYWORDS: topological Kondo insulator, periodic Anderson model, antiferromagnetic topological insulator, spin-selective topological insulator

1. Introduction

Since the theoretical discovery of topological insulators (TIs),^{1,2)} topological materials have been the subject of intense theoretical and experimental investigation. Topological materials are characterized by their metallic surface (edge) states protected by topology of the bulk wave function. Quite a few of topological insulators have been found so far in this decade, including topological crystalline insulators.³⁻⁶⁾ Furthermore, closely related issues such as topological superconductors,⁷⁻¹²⁾ Weyl semimetals¹³⁻¹⁸⁾ have also been in the focus of intense interest, and the topology has become ubiquitous in condensed matter physics.

Recently, the notion of TIs has been extended to strongly correlated systems, such as the topological Kondo insulator.^{19,20)} In particular, SmB_6 ^{21,22)} has attracted much attention as a promising candidate for the topological Kondo insulator. This compound has been known as a Kondo insulator for a long time since about 40 years ago, and it has been recently proposed that the saturation of its electrical resistivity at low temperatures is due to the topological surface current. In addition to topological Kondo insulators, there are intriguing topological phenomena²³⁻³⁵⁾ under electron correlations such as topological Mott insulators,³⁶⁻³⁹⁾ interaction-reduced classifications,⁴⁰⁻⁵⁸⁾ the competition between long-range-ordered phases and TIs.⁵⁹⁻⁷³⁾ The strong correlation effects on topological states are particularly interesting because of nontrivial properties originating from the interplay between topology and correlation.

In this paper, we focus on the topological properties in long-range ordered phases such as ferromagnetic (FM) and antiferromagnetic (AFM) phases. The emergence of topological properties in the magnetic phases has already been studied. For example, the antiferromagnetic topological insulator (AFTI)⁵⁹⁾ has been proposed for three-dimensional (3D) systems. In such AFTIs, the

translation symmetry is broken and the unit cell is doubled. The antiferromagnetic order breaks time-reversal (Θ) and primitive-lattice translational ($T_{1/2}$) symmetries, but preserves their combined symmetry $S = T_{1/2}\Theta$. Under this symmetry, the system has a Z_2 topological number, which is related to the strong index of 3D topological insulators. We note, however, that this Z_2 number is allowed only for 3D systems, as confirmed by the periodic table.⁷⁴⁻⁷⁷⁾ We here challenge this problem, and demonstrate that we can realize the AFTI even in two-dimensional (2D) systems, by taking into account a mirror symmetry.

Concerning nontrivial properties in the ferromagnetic phases, a spin-selective topological insulator (SSTI) was proposed for heavy-fermion systems.⁶⁶⁾ This is a half-metallic ferromagnetic phase⁷⁸⁻⁸²⁾ around quarter filling where one spin sector acquires a gap while the other remains gapless, which is called spin-selective gap. If the insulating sector has a nontrivial topological number, we have the SSTI, which is a unique topological insulator embedded in a metallic phase. Unfortunately, however, this phase is shown to emerge only in the spin conserving systems, and is not compatible generally with the presence of spin-orbit coupling that is necessary for topological properties. Here, we will overcome this difficulty, and propose a way to realize a SSTI for a spin nonconserving system in the presence of spin-orbit coupling.

We explore the above-mentioned topological states in 2D magnetically ordered phases by using an effective model of the topological Kondo insulator for heavy-fermion systems, and demonstrate how they can emerge by using the Hartree-Fock (HF) approximation. Our main idea to realize such topological states in 2D magnetic phases is to take into account crystal symmetries, in particular, a mirror symmetry. We address two kinds of magnetic phases; a 2D antiferromagnetic phase at half filling and a half-metallic ferromagnetic phase around quarter filling. By taking into account the mirror sym-

*E-mail address: kimura.kazuhiro.85n@st.kyoto-u.ac.jp

metry, we elucidate the remarkable facts that a 2D antiferromagnetic phase can have topologically nontrivial structure specified by a mirror Chern number, and a half-metallic ferromagnetic phase can have a topologically nontrivial structure specified by a Chern number. An important point is that these states can appear for spin nonconserving systems.

The rest of this paper is organized as follows. In Sec. 2, we introduce the model and the method. We then discuss the results about the antiferromagnetic topological insulator at half filling in Sec. 3.1, and the half-metallic ferromagnetic topological insulator near quarter filling in Sec. 3.2. In Sec. 3.3, we briefly address the electron correlation effect on our topological phases. A brief summary is given in Sec. 4.

2. Model and Method

We explore the topological properties of the heavy-fermion systems by employing a 2D periodic Anderson model with nonlocal d - f hybridization.^{19,20,83,84} Specifically, we analyze the following topological periodic Anderson model showing band inversion at X points^{29,32,85,86} due to next nearest neighbor (n.n.n.) hopping which is important for describing SmB₆. Here, we note that d -electrons are conduction electrons. In addition to the strong interaction U_f between f -electrons, we also consider the interaction U_d between d -electrons. The Hamiltonian reads

$$H = \sum_{\mathbf{k}} \begin{pmatrix} d_{\mathbf{k}}^{\dagger} & f_{\mathbf{k}}^{\dagger} \end{pmatrix} \begin{pmatrix} \epsilon_{\mathbf{k}}^d & V_{\mathbf{k}} \\ V_{\mathbf{k}}^{\dagger} & \epsilon_{\mathbf{k}}^f \end{pmatrix} \begin{pmatrix} d_{\mathbf{k}} \\ f_{\mathbf{k}} \end{pmatrix} + \sum_{j;\alpha=(d,f)} U_{\alpha} n_{j\uparrow}^{\alpha} n_{j\downarrow}^{\alpha}, \quad (1a)$$

with

$$\epsilon_{\mathbf{k}}^d = [-2t_d(\cos k_x + \cos k_y) - 4t'_d \cos k_x \cos k_y] \sigma_0, \quad (1b)$$

$$\epsilon_{\mathbf{k}}^f = [\epsilon_f - 2t_f(\cos k_x + \cos k_y) - 4t'_f \cos k_x \cos k_y] \sigma_0, \quad (1c)$$

$$V_{\mathbf{k}} = -2[\sigma_x \sin k_x (V_1 + V_2 \cos k_y) + \sigma_y \sin k_y (V_1 + V_2 \cos k_x)], \quad (1d)$$

where $\epsilon_{\mathbf{k}}^d(\epsilon_{\mathbf{k}}^f)$ is the dispersion of d -(f -) electrons, $V_{\mathbf{k}}$ is a Fourier component of the nonlocal d - f hybridization, and \mathbf{k} is a wave number. The annihilation operators are defined as $\mathbf{d}_{\mathbf{k}} = (d_{\mathbf{k}\uparrow} \ d_{\mathbf{k}\downarrow})^T$, $\mathbf{f}_{\mathbf{k}} = (f_{\mathbf{k}\uparrow} \ f_{\mathbf{k}\downarrow})^T$. The basis function for this model is $(d_{\uparrow}, d_{\downarrow}, f_{\uparrow}, f_{\downarrow})^T$, where σ_i ($i = 0, x, y, z$) are the Pauli matrices for spins. Here, t_d , t_f , t'_d and t'_f are hopping parameters, and V_1 and V_2 denote the d - f hybridization, and ϵ_f is the difference between d - and f -electron energies. We consider the above model on a 2D square lattice in the x - y plane, which is a 2D version of the topological crystalline insulator in a 3D cubic lattice. The system has inversion symmetry, so that the hybridization has odd parity, $V_{\mathbf{k}} = -V_{-\mathbf{k}}$.

In order to study the ground state of the model in Eqs. (1), we employ the HF approximation for the Coulomb

term as

$$n_{i\uparrow}^{\alpha} n_{i\downarrow}^{\alpha} \sim n_{i\uparrow}^{\alpha} \langle n_{i\downarrow}^{\alpha} \rangle + \langle n_{i\uparrow}^{\alpha} \rangle n_{i\downarrow}^{\alpha} - \langle n_{i\uparrow}^{\alpha} \rangle \langle n_{i\downarrow}^{\alpha} \rangle, \quad (2)$$

where $n_{i\sigma}^{\alpha}$ ($\alpha = d, f$) is the number operator. Here, $\langle \dots \rangle$ denotes the expectation value at zero temperature.

We introduce the mirror operation M_z , which inverts the z -axis as,

$$M_z = i \tau_z \otimes \sigma_z, \quad (3)$$

where τ_i ($i = 0, x, y, z$) specifies d - and f -electrons. In order to consider the magnetically ordered topological insulating states with a mirror symmetry, we introduce the corresponding topological number. First, recall that the Chern number in multiband systems is given as,

$$C = \frac{1}{2\pi} \sum_i \int_S [\nabla_{\mathbf{k}} \times \mathcal{A}_i]_z dk_x dk_y, \quad (4)$$

where $\mathcal{A}_i(\mathbf{k}) = -i \langle u_i(\mathbf{k}) | \nabla_{\mathbf{k}} | u_i(\mathbf{k}) \rangle$ is the $U(1)$ Berry connection, where $|u_i(\mathbf{k})\rangle$ is a Bloch state with a occupied band index i , which is an eigenstate of $\mathcal{H}(\mathbf{k})$. In the mirror-symmetric system, all the eigenstates are characterized by their mirror parities and divided into two subspaces as,

$$\mathcal{H}(\mathbf{k}) = \begin{pmatrix} \mathcal{H}_{M_z=+i}(\mathbf{k}) & 0 \\ 0 & \mathcal{H}_{M_z=-i}(\mathbf{k}) \end{pmatrix}. \quad (5)$$

The net Chern number C and the mirror Chern number C_m are defined by the Chern numbers $C_{\pm i}$ obtained in each mirror subspace, namely,

$$C = C_{M_z=+i} + C_{M_z=-i}, \quad (6a)$$

$$C_m = (C_{M_z=+i} - C_{M_z=-i})/2. \quad (6b)$$

3. Results

We here discuss the obtained results for the magnetic phases at half filling and around quarter filling separately. Concrete values of parameters we employ in the following are $t_d = 1$ (energy unit), $t'_d = -0.5$, $t_f = -t_d/5$, $t'_f = -t'_d/5$, $U_d = 2$. Unless otherwise noted we set $(V_1, V_2) = (0.1, -0.4)$. The choice of these parameters will be explained below. The magnetic properties of the system are studied by the HF method and the Chern number is calculated by Fukui-Hatsugai method,⁸⁷ which gives an efficient way for numerical calculations.

3.1 Antiferromagnetic phase

For a heavy-fermion system at half filling, there are an antiferromagnetic phase and a Kondo insulating phase in the ordinary Doniac phase diagram. In contrast to the previous study,⁵⁹ we here demonstrate that the AFTI can emerge in 2D mirror-symmetric systems. The model we employ here is a topological mirror Kondo insulator introduced in Refs 83,84,88, which is a mirror-symmetric extension of the topological Kondo insulator. This model was previously used to address a nonmagnetic Kondo insulating phase. The net Chern number is zero, $C = 0$, because of the time-reversal symmetry, but there is still a possibility of having non-zero mirror Chern number $C_m \neq 0$. We elucidate below that the system can change from a paramagnetic phase to an antiferromagnetic phase

without breaking a mirror symmetry, thus leading to the AFTI. The antiferromagnetic phase, where the magnetization is along the z -axis in our case, breaks a space translation symmetry $T_{1/2}$, and thus the period of the unit cell is doubled. Time reversal symmetry is also broken by the magnetization, but we show that the net Chern number is zero by using the combined symmetry $S = \Theta T_{1/2}$ of time reversal Θ and primitive-lattice translation $T_{1/2}$.

We assume that the nesting vector is $\mathbf{Q} = (\pi, \pi)$ for the antiferromagnetic phase, which is justified for $(t'_d, t'_f, V_2) = (0, 0, 0)$, see below. The mean-field Hamiltonian is given by

$$\mathcal{H}_{\mathbf{k}}^{mf} = \begin{pmatrix} \epsilon_{\mathbf{k}}^d + h_{int}^d & V_{\mathbf{k}} \\ V_{\mathbf{k}}^\dagger & \epsilon_{\mathbf{k}}^f + h_{int}^f \end{pmatrix}, \quad (7a)$$

with

$$\epsilon_{\mathbf{k}}^d = [-2t_d(\cos k_x + \cos k_y)\eta_x - 4t'_d \cos k_x \cos k_y \eta_0]\sigma_0, \quad (7b)$$

$$\epsilon_{\mathbf{k}}^f = [\epsilon_f \eta_0 - 2t_f(\cos k_x + \cos k_y)\eta_x - 4t'_f \cos k_x \cos k_y \eta_0]\sigma_0, \quad (7c)$$

$$V_{\mathbf{k}} = -2[\sin k_x \cdot \sigma_x (V_1 \eta_x + V_2 \eta_0 \cos k_y) + \sin k_y \cdot \sigma_y (V_1 \eta_x + V_2 \eta_0 \cos k_x)], \quad (7d)$$

$$h_{int}^\alpha = U_\alpha \begin{pmatrix} \langle n_{0\downarrow}^{A\alpha} \rangle & 0 & 0 & 0 \\ 0 & \langle n_{0\downarrow}^{B\alpha} \rangle & 0 & 0 \\ 0 & 0 & \langle n_{0\uparrow}^{A\alpha} \rangle & 0 \\ 0 & 0 & 0 & \langle n_{0\uparrow}^{B\alpha} \rangle \end{pmatrix}, \quad (7e)$$

where $\alpha = d, f$, and $\eta_i (i = 0, x, y, z)$ are the Pauli matrices for sublattice indices. The basis function is $(d_{\uparrow}^A, d_{\uparrow}^B, d_{\downarrow}^A, d_{\downarrow}^B, f_{\uparrow}^A, f_{\uparrow}^B, f_{\downarrow}^A, f_{\downarrow}^B)^T$. The mirror operation in the sublattice is

$$M_z = i\tau_z \otimes \sigma_z \otimes \eta_0. \quad (8)$$

3.1.1 The case of $(t'_d, t'_f, V_2) = (0, 0, 0)$

In order to see the essence of the results more clearly, we start with a simplified model having only n.n. hopping and hybridization, i.e. $(t'_d, t'_f, V_2) = (0, 0, 0)$. We first determine the easy axis of the magnetization by using the second-order perturbation theory in the strong correlation limit. As a result, we conclude that the z -direction is the easy axis. The detail for the derivation is given in Appendix A. It turns out that magnetic moments of f - and d -electrons align anti-parallel at each site in the z -direction, as shown in Fig. 1(a).

The mean-field results for $(U_d, V_1) = (2.0, 0.1)$ are summarized in Fig. 1 (b)-(d). Note that the results are not sensitive to the values of V_1 . We obtain an AFTI phase as shown in Fig. 1(b). At $U_f = 2.72$, there is a first-order magnetic phase transition, and the spin configuration in Fig. 1(a), where d - and f -electrons align in the opposite directions, is in accordance with the second-order perturbation analysis. We show the direct and indirect gap in Fig. 1(c). The former is important to determine the topological structure, and we confirm that there is indeed a finite direct gap in the AFM phase. It is seen that the

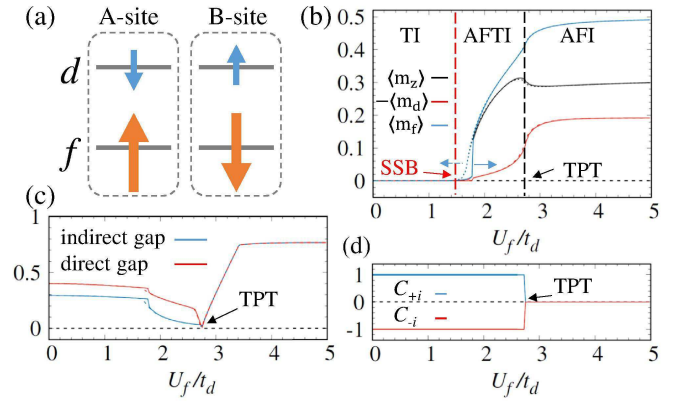


Fig. 1. Magnetic and topological properties for a simplified model with only n.n. hopping and interaction, $(t'_d, t'_f, V_2) = (0, 0, 0)$ and $(U_d, V_1) = (2.0, 0.1)$, obtained with the Hartree-Fock approximation: (a) spin configuration of the AFM phase, (b) staggered magnetic moments, (c) indirect gap and direct gap, (d) Chern number for each sector. In (b), the red dashed line denotes a spontaneous symmetry breaking (SSB) transition, the black dashed line denotes a topological phase transition (TPT) and there is a small hysteresis loop, because of the first-order transition. In (c), the indirect gap is a band gap between conduction and valence bands $\min(E_{\mathbf{k}}^{\text{conduction}} - E_{\mathbf{k}'}^{\text{valence}})$ (\mathbf{k} is not necessarily equal to \mathbf{k}') while the direct gap is the band gap between at wavenumber \mathbf{k} $\min(E_{\mathbf{k}}^{\text{conduction}} - E_{\mathbf{k}}^{\text{valence}})$ and $\text{indirectgap} \leq \text{directgap}$. We have a topological insulator (TI) for $U_f < 1.42$, an AFTI for $1.42 < U_f < 2.72$, an AF trivial insulator (AFI) for $2.72 < U_f$. Everywhere without $U_f = 2.72$, the system is an insulator because of the finite indirect gap.

AFTI phase extends between $U_f = 1.42$ and $U_f = 2.72$, where the mirror Chern number takes $C_m = 1$ in Fig. 1(d) with the finite magnetization in Fig. 1(b). In the strong interaction region, there is a topological phase transition to a trivial phase at $U_f = 2.72$, where both of direct and indirect gaps are closed. As seen from Fig. 1(d), the transition is accompanied by the change of the mirror Chern number from $C_m = 1$ to $C_m = 0$ while the net Chern number is zero. This topological phase transition is triggered by the competition between two types of gap. Namely, in the weak interaction region the topologically nontrivial gap due to the nonlocal hybridization V_1 is dominant, while in the strong interaction region, the topologically trivial gap with the AFM order is dominant. The competition between the two different states gives rise to the topological phase transition accompanied by a gap closing.

3.1.2 The case of $(t'_d, t'_f, V_2) = (-0.5, 0.1, -0.4)$

We now investigate the model with a specific choice of the parameters, $(t'_d, t'_f, V_2) = (-0.5, 0.1, -0.4)$. Importantly, these parameters can describe band inversions for the X points in the three-dimensional Brillouin Zone (see Appendix B), leading to a strong topological insulator phase, as observed for SmB_6 via ARPES measurements.^{21,22} The results obtained for topological and magnetic properties at half filling are shown in Fig. 2(a). A prominent feature in this model is that the system becomes metallic where the indirect gap is closed in the AFM phase even at half filling, as seen in Fig. 2(b). Note, however, that the topological properties still remain in-

tact in this region because the direct gap is not closed. Namely, the Chern number is still well-defined (Fig. 2(c)) in the region where the direct gap is open. Thus, the topological properties remain even in a "metal", and such a metal adiabatically connected to topological insulator is called a topological semimetal. We note that this definition of semimetal is standard in condensed matter, but slightly different from Dirac/Weyl semimetals which are zero-gap semiconductors by definition. Finally, there are several topological phase transitions between different Chern numbers, as seen in Fig. 2(c). This spin configuration is of AFM-II type in Fig. 2(d).

Summarizing all these results, we end up with the phase diagram shown in Fig. 3. The vertical axis denotes the strength of interaction U_f and horizontal axis the strength of hybridization V_1 . There are two antiferromagnetic phases in Fig. 2(d). The above analysis on the blue line ($V_1 = 0.1, V_2 = -0.4$) is included in the region $|V_1| > |V_2|$ where the spin configuration is of AFM-II type. In the antiferromagnetic phase in these parameters, a semimetallic AFM topological phase is realized, which we refer to as an antiferromagnetic topological semimetal. The mirror Chern number has various values in the phase diagram, which is due to the presence of n.n.n. hopping and hybridization, and enriched by U_d . For reference, in Appendix C, we show the phase diagram for $U_d = 0$, which is much simpler than the one discussed above.

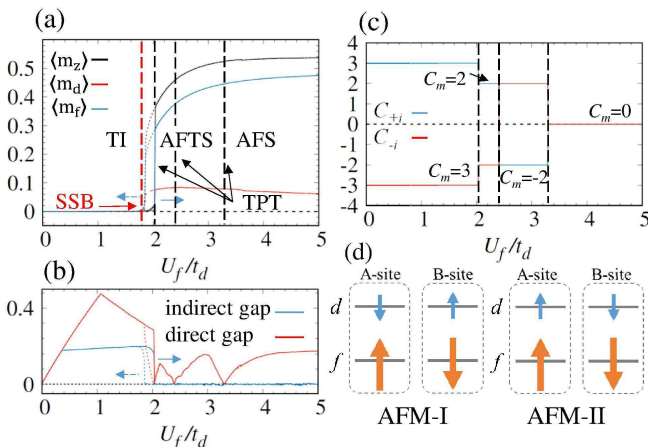


Fig. 2. Magnetic and topological properties for the effective model of SmB₆, $(t'_d, t'_f, V_2) = (-0.5, 0.1, -0.4)$ and $(U_d, V_1) = (2.0, 0.1)$ at half filling: (a) staggered magnetic moments, (b) indirect gap and direct gap, (c) Chern number for each sector, (d) spin configurations of the two AFM phases. In (a), there is a small hysteresis loop, because of the first-order transition. In (b), the region where the indirect gap is closed is semimetallic, and the points where the direct gap is closed denote the topological phase transitions. In (c), there are two Chern numbers for two mirror sectors and the change of the Chern numbers signals the topological phase transition. We have an AF topological semimetal (AFSM) for $1.8 < U_f < 3.25$ and an AF trivial semimetal (AFS) for $U_f < 3.25$.

Here some comments are in order on the difference between the current results and the previous ones. So far, topological properties with the AFM order have been studied in Refs. 61–65, focusing on the systems with

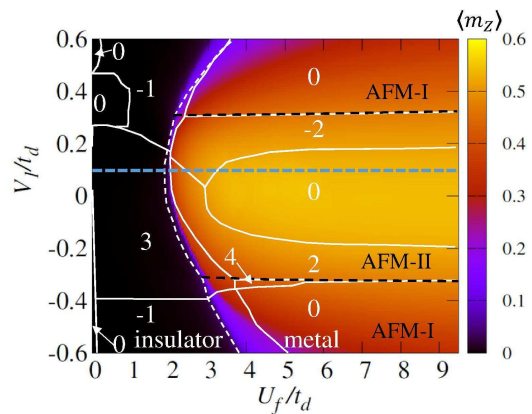


Fig. 3. Phase diagram of mirror-symmetric AFTI at half filling for $U_d = 2$, as functions of the interaction U_f and the hybridization V_1 . The white (dashed) line denotes the topological (insulator-metal) phase transition line, and the black dashed line separates two AFM phases, i.e. AFM-I and AFM-II. We set $V_2 = -0.4$. In the metallic region, the indirect gap is closed, so that there is the Fermi surface. However, the direct gap at the same wave number \mathbf{k} is not closed, so that the Chern number is still well-defined. The white numbers are mirror Chern numbers. The mirror Chern numbers take 4, 3, 2, 0, -1, -2 in this figure.

spin $U(1)$ symmetry. In the presence of the spin-orbit coupling, however, such $U(1)$ symmetry may disappear generally. Here, we stress that the AFTI in our analysis is more generic in the sense that our scenario does not require spin $U(1)$ symmetry. Antiferromagnetic systems respecting mirror symmetry with strong spin-orbit coupling will be candidates for the AFTI proposed in this paper.

3.2 Ferromagnetic phase

We now move to an intriguing topological half-metallic state. Around quarter filling in the Kondo lattice system, it has been known that a half-metallic ferromagnetic phase dubbed a spin-selective Kondo insulator^{78–82)} appears, where a spin-selective gap opens, namely, one spin sector is metallic while the other is insulating. This has been demonstrated for spin conserving systems, and has been extended later to a topological version referred to as a spin-selective topological insulator (SSTI)⁶⁶⁾ where the insulating sector has topologically nontrivial properties. A crucial problem in the previous proposals is that all the results on the SSTI rely on spin $U(1)$ symmetry, which would disappear in the presence of spin-orbit coupling in general. Thus, one might naively think that the SSTI cannot appear in reality. To overcome this difficulty, we here demonstrate that by using a mirror symmetry such a topological half-metallic state can indeed exist in the 2D ferromagnetic phase.

In Figs. 4 and 5, we show the results obtained around quarter filling. At filling of 0.335 and $U_d = 0$, a ferromagnetic phase emerges, as seen in Fig. 4(a), where the magnetization has a hysteresis loop. From density of states (DOS) shown in Fig. 4(b), we find that the system is metallic at $U_f = 0$, whereas the system is half-metallic at $U_f = 4$ with the $M_z = +i$ sector being metallic while the $M_z = -i$ sector insulating, as seen in Fig. 4(c). This

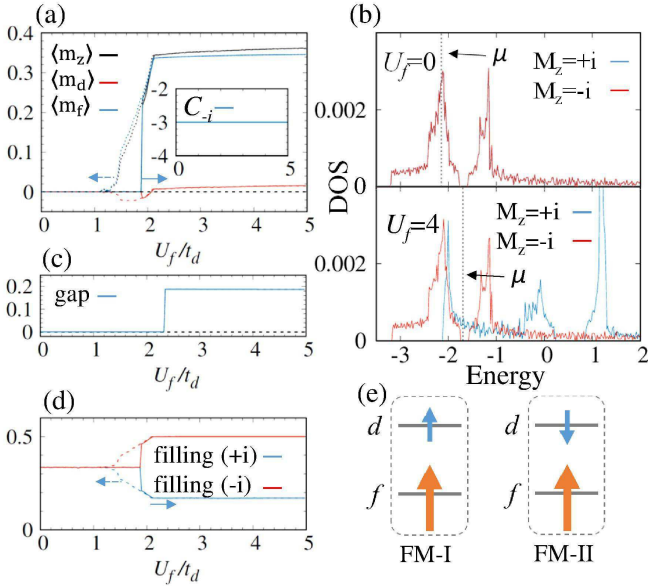


Fig. 4. Magnetic and topological properties around quarter filling for $(U_d, U_f) = (0, 4)$ and filling of 0.335: (a) magnetization of f - (d -) electrons, where the Chern number for the gapped sector is plotted in the inset. (b) DOS at $U_f = 0$ and $U_f = 4$, (c) gap of insulating sector, (d) electron filling for each mirror sector, (e) spin configurations. In (a), the red (blue) line represents d - (f -) electron magnetization and the black line the total magnetization. For all U_f , the system has the same Chern number $C_{-i} = -3$ in the mirror sector $M_z = -i$. In (b), we show the DOS for the sector of $M_z = +i$ ($M_z = -i$) by the blue (red) line, where the chemical potential μ is indicated by the dashed black line. In (c), the blue line is a gap of the mirror sector $M_z = -i$. In the region of $U_f > 2.3$, the sector $M_z = -i$ is an insulator. We have a metallic state at $U_f = 0$, while at $U_f = 4$, we have the SSTI where the sector $M_z = +i$ ($M_z = -i$) is a metal (an insulator).

mirror selective gap gives rise to a nontrivial topological number $C_{-i} = -3$ in Fig. 4(a), resulting in a mirror-selective topological insulator where the filling of the insulating sector is always half, as seen in Fig. 4(d). This spin configuration is of FM-I type in Fig. 4(e).

All these results are put together in the phase diagram of Fig. 5 shown as functions of the strength of interaction U_f and the filling in the system. There are two ferromagnetic phases having different types of spin configuration in Fig. 4(e) and the system has the competition of two magnetic orders. We also study the case including the finite interaction U_d , as shown in Appendix D. At $U_d = 2$, there is no topological phase, in contrast to the above-mentioned case of $U_d = 0$ in Fig. 5, which shows a nontrivial topological phase in some parameter region. Summarizing, we find the mirror-selective topological insulator in a half-metallic ferromagnetic phase, which can emerge for spin nonconserving systems, in contrast to the previous proposals.

3.3 Electron correlation effect

So far, we have discussed the nontrivial topological states in the antiferromagnetic phase and the half-metallic ferromagnetic phase in the HF approximation. One may ask what will happen if electron correlations are taken into account beyond the HF treatment. Here, we argue that the topological properties obtained from

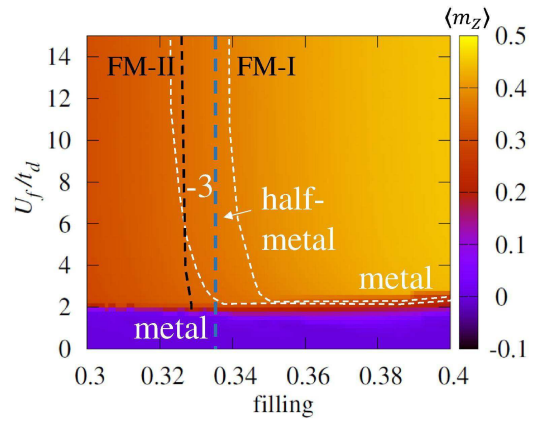


Fig. 5. Phase diagram of mirror-selective topological insulator around quarter filling for $U_d = 0$. The white dashed line denotes the insulator-metal phase transition line, and the black dashed line separates two FM phases, i.e. FM-I and FM-II. In the half-metallic region, the sector $M_z = -i$ has a finite gap and the sector $M_z = +i$ is metallic. The white numbers are mirror Chern numbers of the sector $M_z = -i$ in the whole region. The blue dashed line represent the filling of 0.335.

the mean-field Hamiltonian can persist even if we consider electron correlations by e.g. dynamical mean field theory, as far as the Mott transition is absent. Recall that the Chern number of each mirror sector is given in terms of the Green's function as,

$$C_\sigma = \int \frac{d\omega d^2k}{24\pi^2} \text{Tr}[\epsilon^{\mu\nu\rho} G_\sigma \partial_\mu G_\sigma^{-1} G_\sigma \partial_\nu G_\sigma^{-1} G_\sigma \partial_\rho G_\sigma^{-1}], \quad (9)$$

where $\epsilon_{\mu\nu\rho}$ is totally antisymmetric Levi-Civita tensor, $(\partial_0, \partial_1, \partial_2) = (\partial_\omega, \partial_{k_x}, \partial_{k_y})$, $k = (\omega, \mathbf{k})$. Summation is assumed over repeated indices $\mu, \nu, \rho = 0, 1, 2$. σ specifies mirror parity, and G_σ is the full single-particle Green's function that is related to the free Green's function $G_{\sigma 0}$ via $G_\sigma^{-1}(i\omega, \mathbf{k}) = G_{\sigma 0}^{-1}(i\omega, \mathbf{k}) - \Sigma_\sigma(i\omega, \mathbf{k})$, where $\Sigma_\sigma(i\omega, \mathbf{k})$ is the self-energy. In the present treatment, G_σ is a 4×4 (2×2) matrix in the AFM (half-metallic FM) case. According to Refs. 89–92, the Chern number is determined by the topological Hamiltonian $h_\sigma^{\text{eff}}(\mathbf{k}) = -G_\sigma^{-1}(0, \mathbf{k}) = -G_{\sigma 0}^{-1}(0, \mathbf{k}) + \Sigma_\sigma(0, \mathbf{k})$. This is because the Chern number does not change under the smooth deformation as,

$$G_\sigma(i\omega, \mathbf{k}, \lambda) = (1 - \lambda)G_\sigma(i\omega, \mathbf{k}) + \lambda[i\omega + G_\sigma^{-1}(0, \mathbf{k})]^{-1}, \quad (10)$$

where $\lambda \in [0, 1]$, as far as $\det G_\sigma \neq 0$ and $\det G_\sigma^{-1} \neq 0$ are satisfied. The cases of $\det G_\sigma = 0$ and $\det G_\sigma^{-1} = 0$ respectively correspond to the gap closing or the emergence of Mott insulators with $\text{Im}[\Sigma(0, \mathbf{k})] \rightarrow -\infty$. Therefore, as far as the Mott transition does not occur, the electron correlation effect on the AFM (half-metallic FM) phase can be treated with the renormalized band insulator, and thus the HF results may not be changed qualitatively, although the phase diagram should be modified quantitatively.

4. Summary

We have explored two topological states in the anti-ferromagnetic/ferromagnetic phases by taking account of the mirror symmetry in heavy-fermion systems. Concretely, in reference to topological crystalline insulators, we have proposed 2D topological crystalline insulating states in magnetic phases for interacting systems. In particular, we have shown that in the antiferromagnetic phase at half filling there is a topological state characterized by a mirror Chern number. In the case of a SmB₆ film, an antiferromagnetic topological semimetallic phase should be expected. We have also shown that in the half-metallic ferromagnetic phase around quarter filling, the spin-selective topological insulating state characterized by a mirror Chern number is realized.

In contrast to the previous studies which assumed spin $U(1)$ symmetry to obtain such topological properties in the magnetic phases, our proposal is that these phases can be realized even in the absence of spin $U(1)$ symmetry by taking into account crystalline symmetry in magnetic phases. Generally, spin $U(1)$ symmetry is not preserved in the presence of spin-orbit coupling, so that the present scenario without respecting spin $U(1)$ symmetry will provide a feasible platform to realize magnetic topological insulators for two-dimensional systems.

In this paper, we have employed the HF approximation to address the above phases. We have discussed the correlation effects qualitatively, and shown that topological properties of these states may not change in the presence of correlation effects. Nevertheless, more elaborate calculations should be done to confirm this conclusion, which is now under consideration. In addition, a three-dimensional version of the mirror-selective topological insulator is discussed.⁹³⁾ It might be interesting to study how our mirror-selective topological insulator extends to three dimensions by increasing thickness of the layers.

Acknowledgments

We thank R. Peters for fruitful discussion. This work is partly supported by JSPS KAKENHI Grant No. JP15H05855 and No. JP16K05501. The numerical calculations were performed on supercomputer at the ISSP in the University of Tokyo, and the SR16000 at YITP in Kyoto University.

Appendix A: Spin configurations in strong correlation limit

In this Appendix, we determine the magnetization axis by using the second-order perturbation theory to clarify whether the magnetization is mirror-symmetric or not. For simplicity, we use the model with $V_2 = 0$, $t'_d = 0$, $t'_f = 0$ at half filling. Starting from the strong correlation limit $U_f \gg 1$, we use the normalized hybridization V_1/U_f as a perturbation parameter. We use the following relations between spins S_i^α ($\alpha = d, f$ and $i = x, y, z$) of d -/ f -electrons and fermionic operators $d_{i\sigma}$ and $f_{j\sigma}$ with spin indices $\sigma = \uparrow, \downarrow$ and site indices i, j ,

$$S_{xi}^d \cdot S_{xj}^f = \frac{1}{2} \sum_{\sigma=\uparrow,\downarrow} \left(d_{i\sigma}^\dagger d_{i\bar{\sigma}} f_{j\sigma}^\dagger f_{j\bar{\sigma}} + d_{i\sigma}^\dagger d_{i\bar{\sigma}} f_{j\bar{\sigma}}^\dagger f_{j\sigma} \right),$$

$$(A.1a)$$

$$S_{yi}^d \cdot S_{yj}^f = \frac{1}{2} \sum_{\sigma=\uparrow,\downarrow} \left(-d_{i\sigma}^\dagger d_{i\bar{\sigma}} f_{j\sigma}^\dagger f_{j\bar{\sigma}} + d_{i\sigma}^\dagger d_{i\bar{\sigma}} f_{j\bar{\sigma}}^\dagger f_{j\sigma} \right),$$

$$(A.1b)$$

$$S_{zi}^d \cdot S_{zj}^f = \frac{1}{2} \sum_{\sigma=\uparrow,\downarrow} \left(d_{i\sigma}^\dagger d_{i\sigma} f_{j\sigma}^\dagger f_{j\sigma} - d_{i\sigma}^\dagger d_{i\sigma} f_{j\bar{\sigma}}^\dagger f_{j\bar{\sigma}} \right),$$

$$(A.1c)$$

$$n_i^d \cdot n_j^f = \sum_{\sigma=\uparrow,\downarrow} \left(d_{i\sigma}^\dagger d_{i\sigma} f_{j\sigma}^\dagger f_{j\sigma} + d_{i\sigma}^\dagger d_{i\sigma} f_{j\bar{\sigma}}^\dagger f_{j\bar{\sigma}} \right).$$

$$(A.1d)$$

The hybridization term then results in the exchange interaction via the second-order perturbation as,

$$\begin{aligned} H' &= \sum_{i \in x} J_{df}^{ix} S_{xi}^d \cdot S_{xi-1}^f + J_{df}^{iy} S_{yi}^d \cdot S_{yi-1}^f + J_{df}^{iz} S_{zi}^d \cdot S_{zi-1}^f \\ &+ \sum_{i \in x} J_{df}^{ix} S_{xi-1}^d \cdot S_{xi}^f + J_{df}^{iy} S_{yi-1}^d \cdot S_{yi}^f + J_{df}^{iz} S_{zi-1}^d \cdot S_{zi}^f \\ &+ \sum_{j \in y} J_{df}^{jx} S_{xj}^d \cdot S_{xj-1}^f + J_{df}^{jy} S_{yj}^d \cdot S_{yj-1}^f + J_{df}^{jz} S_{zj}^d \cdot S_{zj-1}^f \\ &+ \sum_{j \in y} J_{df}^{jx} S_{xj-1}^d \cdot S_{xj}^f + J_{df}^{jy} S_{yj-1}^d \cdot S_{yj}^f + J_{df}^{jz} S_{zj-1}^d \cdot S_{zj}^f, \end{aligned}$$

$$(A.2)$$

where $J_{df}^{i,\alpha}$ ($i = x, y$ and $\alpha = x, y, z$) are coupling constants between d - and f -electrons. For the spin configuration along the x -axis, the coupling constants read $J_{df}^{ix} = J_{df} > 0$, $J_{df}^{iy} = -J_{df} < 0$, $J_{df}^{iz} = -J_{df} < 0$, while for the y -axis, they read $J_{df}^{jx} = -J_{df} < 0$, $J_{df}^{jy} = J_{df} > 0$, $J_{df}^{jz} = -J_{df} < 0$ in Table. A.1, $J_{df} = 2V_1^2 \left(\frac{1}{\epsilon_f} + \frac{1}{U_f - \epsilon_f} \right) > 0$ and ϵ_f is the chemical potential of f -electrons. From only this constraint, we cannot yet determine the spin configuration at the ground state. When $t_{dd} = t_{ff} = 0$, the spins can be polarized along the x - or the y -direction without energy loss.

We then consider another perturbation expansion in t_f/U_f for $U_f \gg 1$. It induces the antiferromagnetic interaction $J_{ff} \mathbf{S}_i^f \cdot \mathbf{S}_j^f$ ($J_{ff} < 0$), giving rise to frustration in the cases. As a result, the easy axis of the magnetization is the z -axis, preserving the mirror symmetry, and the ground state of this model prefers the configuration having the staggered AFM order in Fig. A-1, where all other magnetic configurations are frustrated. Those for d -electrons and f -electrons align in the opposite directions at the same site.

Table A.1. Exchange couplings obtained for the spin-half 2D periodic Anderson model with nonlocal d - f hybridization using second-order perturbation theory from strong correlation limit. $J_{df}^x, J_{df}^y, J_{df}^z$ are coupling constants for effective spin model, where superscripts x, y and z specify the quantization axis for spin. There are two spin configuration along the x - and y -axis. + (-) means an antiferromagnetic(AF) (ferromagnetic(F)) coupling.

	J_{df}^x	J_{df}^y	J_{df}^z
x - axis	+(AF)	-(F)	-(F)
y - axis	-(F)	+(AF)	-(AF)

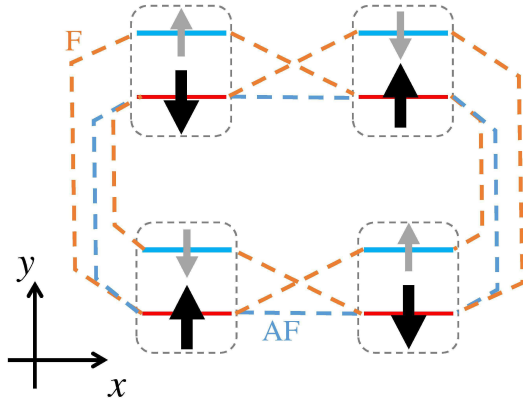


Fig. A.1. Spin configuration in real space, where all the spins align along the z -axis. The blue (red) lines denote d - (f -) level and the bold black/gray arrow denote spins. The dashed blue (orange) lines indicated the antiferromagnetic (ferromagnetic) coupling, where we consider the perturbation in V_1/U_f and t_f/U_f . There is no frustration and the configuration having the staggered AFM is realized and f - and d -electrons align anti-parallel at each site.

We further consider the perturbation expansion in t_d/U_d for $U_d \gg 1$, because d -electrons have reasonably strong correlation. It turns out that this term induces the antiferromagnetic interaction $J_{dd}\mathbf{S}_i^d \cdot \mathbf{S}_j^d$ ($J_{dd} < 0$) with no frustration in this order, if the easy axis of magnetization is the z -axis. In this situation, the coupling constants are modified as $J_{df} = 2V_1^2(\frac{1}{U_d + \epsilon_f} + \frac{1}{U_f - \epsilon_f}) > 0$, but the sign is unchanged. We thus conclude that the easy axis of the magnetization is the z -axis and the staggered AFM, where f - and d -electrons align anti-parallel at each site, is realized.

Appendix B: Three dimensional effective model of SmB_6

Three dimensional effective model Hamiltonian^{83,84,88} reads:

$$H_{\mathbf{k}} = \sum_{\mathbf{k}} \begin{pmatrix} d_{\mathbf{k}}^\dagger & f_{\mathbf{k}}^\dagger \end{pmatrix} \begin{pmatrix} \epsilon_{\mathbf{k}}^d & V_{\mathbf{k}} \\ V_{\mathbf{k}}^\dagger & \epsilon_{\mathbf{k}}^f \end{pmatrix} \begin{pmatrix} d_{\mathbf{k}} \\ f_{\mathbf{k}} \end{pmatrix} \quad (\text{B.1a})$$

with

$$\begin{aligned} \epsilon_{\mathbf{k}}^d &= [-2t_d(\cos k_x + \cos k_y + \cos k_z) \\ &\quad -4t'_d(\cos k_x \cos k_y + \cos k_y \cos k_z \\ &\quad + \cos k_z \cos k_x)]\sigma_0, \end{aligned} \quad (\text{B.1b})$$

$$\epsilon_{\mathbf{k}}^f = [\epsilon_f - 2t_f(\cos k_x + \cos k_y + \cos k_z)$$

$$\begin{aligned} &-4t'_f(\cos k_x \cos k_y + \cos k_y \cos k_z \\ &\quad + \cos k_z \cos k_x)]\sigma_0, \end{aligned} \quad (\text{B.1c})$$

$$\begin{aligned} V_{\mathbf{k}} &= -2[\sigma_x \sin k_x (V_1 + V_2(\cos k_y + \cos k_z)) \\ &\quad + \sigma_y \sin k_y (V_1 + V_2(\cos k_z + \cos k_x)) \\ &\quad + \sigma_z \sin k_z (V_1 + V_2(\cos k_x + \cos k_y))], \end{aligned} \quad (\text{B.1d})$$

where $\epsilon_{\mathbf{k}}^d(\epsilon_{\mathbf{k}}^f)$ is the dispersion of d -(f -) electrons, $V_{\mathbf{k}}$ is a Fourier component of the nonlocal d - f hybridization, and \mathbf{k} is a wave number. The annihilation operators are defined as $\mathbf{d}_{\mathbf{k}} = (d_{\mathbf{k}\uparrow} \ d_{\mathbf{k}\downarrow})^T$, $\mathbf{f}_{\mathbf{k}} = (f_{\mathbf{k}\uparrow} \ f_{\mathbf{k}\downarrow})^T$. The basis function for this model is $(d_{\uparrow}, d_{\downarrow}, f_{\uparrow}, f_{\downarrow})^T$, where σ_i ($i = 0, x, y, z$) are the Pauli matrices for spins. Concrete values of parameters we employ are $t_d = 1$ (energy unit), $t'_d = -0.5$, $t_f = -t_d/5$, $t'_f = -t'_d/5$. Note that this model has three band inversions at X points^{29,32,85,86}) as shown in Fig. B.1. Our two-dimensional effective model is introduced to properly take into account this inversion property.

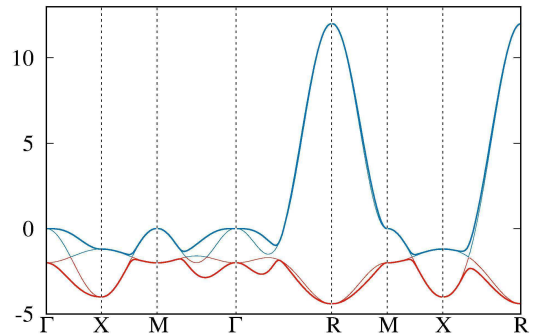


Fig. B.1. (Color line) Energy spectrum of the model for three-dimensional SmB_6 . The thick lines are band structure of d - and f - electrons, $(V_1, V_2) = (0.1, -0.4)$. The thin lines show the bare energies of d and f bands for the same parameters but with vanishing hybridization $(V_1, V_2) = (0, 0)$. The band inversion at the X point is realized.

Appendix C: Antiferromagnetic topological insulator at half filling for $U_d = 0$

We investigate topological and magnetic properties at half filling in the case of $U_d = 0$. The obtained phase diagram is shown in Fig. C.1. In contrast to the case with finite U_d shown in Fig. 3, the phase diagram is much simpler, but we still find the topologically nontrivial region. We note that in the antiferromagnetic phase, the system becomes a topological semimetal, as mentioned in the main text.

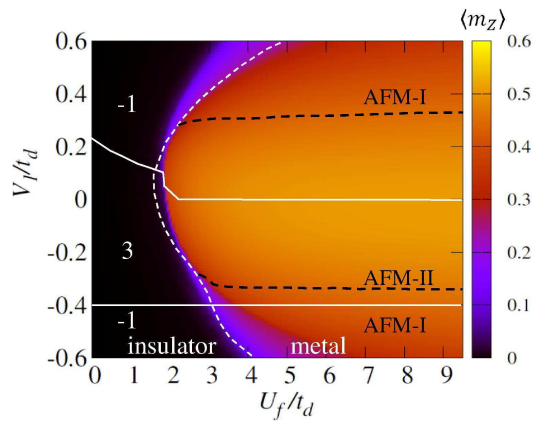


Fig. C-1. Phase diagram of mirror-symmetric AFTI at half filling for $U_d = 0$. The white (dashed) line denotes the topological (insulator-metal) phase transition line. Here, V_1 is the n.n. hybridization and the n.n.n. hybridization $V_2 = -0.4$ is fixed. The white numbers are mirror Chern numbers. In the metallic region, the indirect gap is closed, as mentioned in the main text.

Appendix D: Mirror-selective topological insulator near quarter filling for $U_d = 2$

We investigate topological and magnetic properties around quarter filling in the case of $U_d = 2$. The obtained phase diagram is shown in Fig. D-1. We find that in the ferromagnetic phase, the system is in a half-metallic state but is not topological, in contrast to the finite U_d case shown in Fig. 5

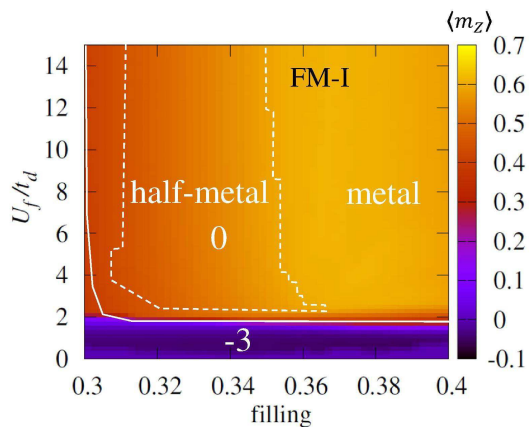


Fig. D-1. Phase diagram of mirror-selective topological insulator around quarter filling for $U_d = 2$. The black line separates the topological phase and trivial phase, while the white line separates the half-metallic phase and the metallic phase. In the half-metallic region, the sector of $M_z = -i$ is an insulator the other sector is a metal. The color plot shows the strength of the magnetization.

- 1) C. L. Kane and E. J. Mele: Phys. Rev. Lett. **95** (2005) 226801.
- 2) C. L. Kane and E. J. Mele: Phys. Rev. Lett. **95** (2005) 146802.
- 3) L. Fu: Phys. Rev. Lett. **106** (2011) 106802.
- 4) T. H. Hsieh, H. Lin, J. Liu, W. Duan, A. Bansil, and L. Fu: Nature communications **3** (2012) 982.
- 5) Y. Tanaka, Z. Ren, T. Sato, K. Nakayama, S. Souma, T. Takahashi, K. Segawa, and Y. Ando: Nature Physics **8** (2012) 800.

- 6) P. Dziawa, B. Kowalski, K. Dybko, R. Buczko, A. Szczerbakow, M. Szot, E. Lusakowska, T. Balasubramanian, B. M. Wojek, M. Berntsen, et al.: Nature materials **11** (2012) 1023.
- 7) A. Y. Kitaev: Physics-Uspekhi **44** (2001) 131.
- 8) V. Mourik, K. Zuo, S. M. Frolov, S. R. Plissard, E. P. A. M. Bakkers, and L. P. Kouwenhoven: Science **336** (2012) 1003.
- 9) L. P. Rokhinson, X. Liu, and J. K. Furdyna: Nature Physics **8** (2012) 795.
- 10) A. Das, Y. Ronen, Y. Most, Y. Oreg, M. Heiblum, and H. Shtrikman: Nature Physics **8** (2012) 887.
- 11) T. Yoshida, M. Sigrist, and Y. Yanase: Phys. Rev. Lett. **115** (2015) 027001.
- 12) A. Daido and Y. Yanase: Phys. Rev. B **94** (2016) 054519.
- 13) S. Murakami: New Journal of Physics **9** (2007) 356.
- 14) X. Wan, A. M. Turner, A. Vishwanath, and S. Y. Savrasov: Phys. Rev. B **83** (2011) 205101.
- 15) A. A. Burkov and L. Balents: Phys. Rev. Lett. **107** (2011) 127205.
- 16) H. Weng, C. Fang, Z. Fang, B. A. Bernevig, and X. Dai: Phys. Rev. X **5** (2015) 011029.
- 17) S.-Y. Xu, I. Belopolski, N. Alidoust, M. Neupane, G. Bian, C. Zhang, R. Sankar, G. Chang, Z. Yuan, C.-C. Lee, S.-M. Huang, H. Zheng, J. Ma, D. S. Sanchez, B. Wang, A. Bansil, F. Chou, P. P. Shibayev, H. Lin, S. Jia, and M. Z. Hasan: Science **349** (2015) 613.
- 18) B. Q. Lv, H. M. Weng, B. B. Fu, X. P. Wang, H. Miao, J. Ma, P. Richard, X. C. Huang, L. X. Zhao, G. F. Chen, Z. Fang, X. Dai, T. Qian, and H. Ding: Phys. Rev. X **5** (2015) 031013.
- 19) M. Dzero, K. Sun, V. Galitski, and P. Coleman: Phys. Rev. Lett. **104** (2010) 106408.
- 20) M. Dzero, J. Xia, V. Galitski, and P. Coleman: Annual Review of Condensed Matter Physics **7** (2016) 249.
- 21) M. Neupane, N. Alidoust, S. Xu, T. Kondo, Y. Ishida, D.-J. Kim, C. Liu, I. Belopolski, Y. Jo, T.-R. Chang, et al.: Nature communications **4** (2013) 2991.
- 22) N. Xu, P. K. Biswas, J. Dil, R. Dhaka, G. Landolt, S. Muff, C. Matt, X. Shi, N. Plumb, M. Radović, et al.: Nature communications **5** (2014) 4566.
- 23) M. Hohenadler, T. C. Lang, and F. F. Assaad: Phys. Rev. Lett. **106** (2011) 100403.
- 24) T. Yoshida, S. Fujimoto, and N. Kawakami: Phys. Rev. B **85** (2012) 125113.
- 25) Y. Tada, R. Peters, M. Oshikawa, A. Koga, N. Kawakami, and S. Fujimoto: Phys. Rev. B **85** (2012) 165138.
- 26) A. Shitade, H. Katsura, J. Kuneš, X.-L. Qi, S.-C. Zhang, and N. Nagaosa: Phys. Rev. Lett. **102** (2009) 256403.
- 27) S. Chadov, X. Qi, J. Kübler, G. H. Fecher, C. Felser, and S. C. Zhang: Nat. Mater. **9** (2010) 541.
- 28) H. Lin, L. A. Wray, Y. Xia, S. Xu, S. Jia, R. J. Cava, A. Bansil, and M. Z. Hasan: Nat. Mater. **9** (2010) 546.
- 29) T. Takimoto: Journal of the Physical Society of Japan **80** (2011) 123710.
- 30) B. Yan, L. Müchler, X.-L. Qi, S.-C. Zhang, and C. Felser: Phys. Rev. B **85** (2012) 165125.
- 31) X. Zhang, N. P. Butch, P. Syers, S. Ziemak, R. L. Greene, and J. Paglione: Phys. Rev. X **3** (2013) 011011.
- 32) F. Lu, J. Zhao, H. Weng, Z. Fang, and X. Dai: Phys. Rev. Lett. **110** (2013) 096401.
- 33) T. H. Hsieh, J. Liu, and L. Fu: Phys. Rev. B **90** (2014) 081112.
- 34) M. Kargarian and G. A. Fiete: Phys. Rev. Lett. **110** (2013) 156403.
- 35) H. Weng, J. Zhao, Z. Wang, Z. Fang, and X. Dai: Phys. Rev. Lett. **112** (2014) 016403.
- 36) D. Pesin and L. Balents: Nat. Phys. **6** (2010) 376.
- 37) T. Yoshida, R. Peters, S. Fujimoto, and N. Kawakami: Phys. Rev. Lett. **112** (2014) 196404.
- 38) T. Yoshida and N. Kawakami: Phys. Rev. B **94** (2016) 085149.
- 39) H.-Q. Wu, Y.-Y. He, Y.-Z. You, T. Yoshida, N. Kawakami, C. Xu, Z. Y. Meng, and Z.-Y. Lu: Phys. Rev. B **94** (2016) 165121.
- 40) L. Fidkowski and A. Kitaev: Phys. Rev. B **81** (2010) 134509.
- 41) L. Fidkowski and A. Kitaev: Phys. Rev. B **83** (2011) 075103.
- 42) A. M. Turner, F. Pollmann, and E. Berg: Phys. Rev. B **83**

- (2011) 075102.
- 43) S. Ryu and S.-C. Zhang: Phys. Rev. B **85** (2012) 245132.
 - 44) H. Yao and S. Ryu: Phys. Rev. B **88** (2013) 064507.
 - 45) X.-L. Qi: New J. Phys. **15** (2013) 065002.
 - 46) Y.-M. Lu and A. Vishwanath: Phys. Rev. B **86** (2012) 125119.
 - 47) M. Levin and A. Stern: Phys. Rev. B **86** (2012) 115131.
 - 48) L. Fidkowski, X. Chen, and A. Vishwanath: Phys. Rev. X **3** (2013) 041016.
 - 49) Z.-C. Gu and X.-G. Wen: Phys. Rev. B **90** (2014) 115141.
 - 50) C.-T. Hsieh, T. Morimoto, and S. Ryu: Phys. Rev. B **90** (2014) 245111.
 - 51) H. Isobe and L. Fu: Phys. Rev. B **92** (2015) 081304.
 - 52) T. Yoshida and A. Furusaki: Phys. Rev. B **92** (2015) 085114.
 - 53) C. Wang, A. C. Potter, and T. Senthil: Science **343** (2014) 629.
 - 54) Y.-Z. You and C. Xu: Phys. Rev. B **90** (2014) 245120.
 - 55) C. Wang and T. Senthil: Phys. Rev. B **89** (2014) 195124.
 - 56) T. Morimoto, A. Furusaki, and C. Mudry: Phys. Rev. B **92** (2015) 125104.
 - 57) T. Yoshida, A. Daido, Y. Yanase, and N. Kawakami: Phys. Rev. Lett. **118** (2017) 147001.
 - 58) T. Yoshida, I. Danshita, R. Peters, and N. Kawakami: arXiv preprint arXiv:1711.09538 (2017).
 - 59) R. S. K. Mong, A. M. Essin, and J. E. Moore: Phys. Rev. B **81** (2010) 245209.
 - 60) A. M. Essin and V. Gurarie: Phys. Rev. B **85** (2012) 195116.
 - 61) S. Okamoto, W. Zhu, Y. Nomura, R. Arita, D. Xiao, and N. Nagaosa: Phys. Rev. B **89** (2014) 195121.
 - 62) H. Guo, S. Feng, and S.-Q. Shen: Phys. Rev. B **83** (2011) 045114.
 - 63) J. He, Y.-H. Zong, S.-P. Kou, Y. Liang, and S. Feng: Phys. Rev. B **84** (2011) 035127.
 - 64) T. Yoshida, R. Peters, S. Fujimoto, and N. Kawakami: Phys. Rev. B **87** (2013) 085134.
 - 65) J. He, B. Wang, and S.-P. Kou: Phys. Rev. B **86** (2012) 235146.
 - 66) T. Yoshida, R. Peters, S. Fujimoto, and N. Kawakami: Phys. Rev. B **87** (2013) 165109.
 - 67) S. Rachel and K. Le Hur: Phys. Rev. B **82** (2010) 075106.
 - 68) C. N. Varney, K. Sun, M. Rigol, and V. Galitski: Phys. Rev. B **82** (2010) 115125.
 - 69) Y. Yamaji and M. Imada: Phys. Rev. B **83** (2011) 205122.
 - 70) D. Zheng, G.-M. Zhang, and C. Wu: Phys. Rev. B **84** (2011) 205121.
 - 71) C. Griset and C. Xu: Phys. Rev. B **85** (2012) 045123.
 - 72) W. Wu, S. Rachel, W.-M. Liu, and K. Le Hur: Phys. Rev. B **85** (2012) 205102.
 - 73) S.-L. Yu, X. C. Xie, and J.-X. Li: Phys. Rev. Lett. **107** (2011) 010401.
 - 74) A. P. Schnyder, S. Ryu, A. Furusaki, and A. W. W. Ludwig: Phys. Rev. B **78** (2008) 195125.
 - 75) A. Kitaev: AIP Conference Proceedings **1134** (2009) 22.
 - 76) S. Ryu, A. P. Schnyder, A. Furusaki, and A. W. W. Ludwig: New Journal of Physics **12** (2010) 065010.
 - 77) K. Shiozaki, M. Sato, and K. Gomi: Phys. Rev. B **93** (2016) 195413.
 - 78) K. S. D. Beach and F. F. Assaad: Phys. Rev. B **77** (2008) 205123.
 - 79) R. Peters, N. Kawakami, and T. Pruschke: Phys. Rev. Lett. **108** (2012) 086402.
 - 80) O. Howczak and J. Spalek: Journal of Physics: Condensed Matter **24** (2012) 205602.
 - 81) R. Peters and N. Kawakami: Phys. Rev. B **86** (2012) 165107.
 - 82) D. Golež and R. Žitko: Phys. Rev. B **88** (2013) 054431.
 - 83) M. Legner, A. Rüegg, and M. Sigrist: Phys. Rev. B **89** (2014) 085110.
 - 84) M. Legner, A. Rüegg, and M. Sigrist: Phys. Rev. Lett. **115** (2015) 156405.
 - 85) M.-T. Tran, T. Takimoto, and K.-S. Kim: Phys. Rev. B **85** (2012) 125128.
 - 86) V. Alexandrov, M. Dzero, and P. Coleman: Phys. Rev. Lett. **111** (2013) 226403.
 - 87) T. Fukui, Y. Hatsugai, and H. Suzuki: Journal of the Physical Society of Japan **74** (2005) 1674.
 - 88) R.-X. Zhang, C. Xu, and C.-X. Liu: Phys. Rev. B **94** (2016) 235128.
 - 89) G. E. Volovik: The universe in a helium droplet (Oxford University Press on Demand, 2003), Vol. 117.
 - 90) V. Gurarie: Phys. Rev. B **83** (2011) 085426.
 - 91) Z. Wang and S.-C. Zhang: Phys. Rev. X **2** (2012) 031008.
 - 92) A. M. Essin and V. Gurarie: Phys. Rev. B **84** (2011) 125132.
 - 93) R. Peters, T. Yoshida, and N. Kawakami, in preparation.